

Efficient and Effective Universal Adversarial Attack against Vision-Language Pre-training Models

Fan Yang

Huazhong University of Science and
Technology
Wuhan, China

Yihao Huang*

Nanyang Technological University
Singapore, Singapore

Kailong Wang*

Huazhong University of Science and
Technology
Wuhan, China

Ling Shi

Nanyang Technological University
Singapore, Singapore

Geguang Pu

East China Normal University
Shanghai, China

Yang Liu

Nanyang Technological University
Singapore, Singapore

Haoyu Wang

Huazhong University of Science and
Technology
Wuhan, China

Abstract

Vision-language pre-training (VLP) models, trained on large-scale image-text pairs, have become widely used across a variety of downstream vision-and-language (V+L) tasks. This widespread adoption raises concerns about their vulnerability to adversarial attacks. Non-universal adversarial attacks, while effective, are often impractical for real-time online applications due to their high computational demands per data instance. Recently, universal adversarial perturbations (UAPs) have been introduced as a solution, but existing generator-based UAP methods are significantly time-consuming. To overcome the limitation, we propose a direct optimization-based UAP approach, termed DO-UAP, which significantly reduces resource consumption while maintaining high attack performance. Specifically, we explore the necessity of multimodal loss design and introduce a useful data augmentation strategy. Extensive experiments conducted on three benchmark VLP datasets, six popular VLP models, and three classical downstream tasks demonstrate the efficiency and effectiveness of DO-UAP. Specifically, our approach drastically decreases the time consumption by 23-fold while achieving a better attack performance.

CCS Concepts

- Computing methodologies → Computer vision;
- Security and privacy → Software and application security.

Relevance. We explore universal adversarial perturbations (UAPs) with a focus on their potential to reveal vulnerabilities in online vision-language applications. By leveraging UAPs' ability to deceive

*Corresponding authors. huangyihao22@gmail.com, wangkl@hust.edu.cn.

Permission to make digital or hard copies of all or part of this work for personal or classroom use is granted without fee provided that copies are not made or distributed for profit or commercial advantage and that copies bear this notice and the full citation on the first page. Copyrights for components of this work owned by others than ACM must be honored. Abstracting with credit is permitted. To copy otherwise, or republish, to post on servers or to redistribute to lists, requires prior specific permission and/or a fee. Request permissions from permissions@acm.org.

Conference acronym 'XX, June 03–05, 2018, Woodstock, NY

© 2018 ACM.

ACM ISBN 978-1-4503-XXXX-X/18/06
<https://doi.org/XXXXXX.XXXXXXX>

neural networks across various image-text pairs without the need for additional overhead, this study underscores critical robustness challenges in these online systems.

1 Introduction

In the evolving web ecosystem, where multimodal content is increasingly prevalent, vision-language pre-training (VLP) models [15, 25, 31, 40] play a crucial role in enhancing user experiences through applications like image search, automatic captioning, and content recommendation. They have transformed multimodal learning by utilizing large-scale image-text pairs to bridge visual and linguistic understanding. Models like CLIP [25], ALBEF [15], and TCL [40] have achieved remarkable results in vision-and-language (V+L) tasks [10, 11, 35, 38]. By employing self-supervised pre-training, these models align cross-modal features, enabling them to capture complex relationships between visual and textual data, thus generating effective multimodal representations.

Despite these advancements, recent research (e.g., Co-Attack, SGA) [20, 43] have identified **critical vulnerabilities in VLP models**, particularly when faced with multimodal adversarial examples. However, these approaches typically rely on generating specific adversarial perturbations for each image-text instance, requiring new perturbations to be learned from scratch. This leads to **significant computational overhead**, limiting the applicability of such attacks in practical scenarios like real-time online applications.

To make the multimodal attack perturbation more practical, designing the universal adversarial perturbation (UAP) method (Fig. 1) is a promising direction. There are two basic UAP generation pipelines: *direct optimization-based* [21] and *generator-based* [24]. Through an empirical study, the recent work CPGC [8] finds the *direct optimization-based* pipeline simply updates UAPs via gradients but often lacks effectiveness. Comparatively, the *generator-based* pipeline is more effective for universally attacking VLP models. As a result, they introduce the first generator-based multimodal UAP designed to mislead VLP models using **fixed, data-agnostic** perturbations. Despite achieving high performance (~90%), the generator-based approach of CPGC is inefficient, demanding significant time and data resources (roughly one week on a single A100 GPU). This

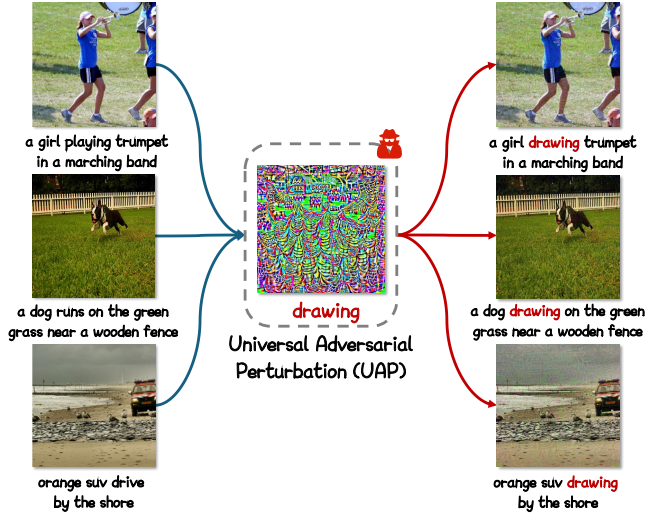


Figure 1: Effect of the universal adversarial perturbations against VLP models. With just a pair of *fixed* image-text perturbations, the proposed attack effectively misleads arbitrary image-text pairs across a wide range of V+L tasks.

inefficiency motivates us to investigate a crucial question: “Can we design a more efficient, direct optimization-based UAP method to achieve comparable effectiveness against VLP models?”

To achieve this, an intuitive idea is to utilize a cross-modal image-text loss to generate UAPs that disrupt the image-text alignment. However, upon further analysis, we reveal that this approach is insufficient due to the “modality gap” phenomenon observed in VLP models [17]. The issue arises because the perturbed image-text pairs remain close to their unperturbed counterparts, which limits their universal effectiveness. To address this limitation, we highlight the necessity of incorporating an unimodal loss alongside the basic cross-modal image-text loss. Additionally, while data augmentations are commonly used to improve adversarial attack performance [20, 37], their impact on UAP attacks remains unclear, and not all augmentations are beneficial for UAP generation. To this end, we introduce an image-text similarity-based idea for selecting useful data augmentations (*i.e.*, brightness). Our approach drastically decreases the time consumption by 23-fold compared to CPGC (state-of-the-art).

To sum up, our work has the following contributions:

- To the best of our knowledge, we propose the first *direct optimization-based* multimodal UAP method targeting VLP models. The approach significantly outperforms generator-based methods, delivering superior attack performance while reducing time consumption.
- We propose a multimodal-oriented loss function and incorporate carefully selected data augmentation, both of which significantly enhance the attack performance of UAP.
- The experimental results on three benchmark VLP datasets, six widely-used VLP models, and three classical downstream tasks strongly affirm the effectiveness of DO-UAP, underscoring the robustness and adaptability of our method across diverse settings.

2 Background and Related Work

2.1 Vision-Language Pre-training Models

Vision-language pre-training (VLP) is a key technique for improving multimodal tasks by utilizing large-scale image-text pairs [5]. Traditionally, research relied on pre-trained object detectors for multimodal representation [15, 40], but Vision Transformers (ViT) [7] have shifted the approach toward end-to-end image encoding, transforming inputs into patches [9].

VLP models are divided into two main types: fused and aligned. Fused models, like ALBEF [15] and TCL [40], use separate unimodal encoders for text and images, followed by a multimodal encoder to combine the embeddings. In contrast, aligned models, such as CLIP [25], use unimodal encoders to independently process image and text embeddings, aligning them for downstream tasks.

For instance, CLIP leverages contrastive learning to align embeddings by maximizing the similarity of matched image-text pairs while minimizing that of unmatched ones. Models like BLIP [14] improve training by synthesizing and filtering captions for web images. Fused models like ALBEF align and then merge unimodal representations using cross-modal attention, while TCL employs contrastive learning to maintain global-local alignment. These pre-trained models show great generalizability and can be fine-tuned for various applications.

2.2 Downstream Vision-and-Language Tasks

Image-Text Retrieval (ITR) involves retrieving relevant information from a database using one modality (image or text) to query the other. It includes image-to-text retrieval (TR) and text-to-image retrieval (IR) [4, 45]. Fused models like ALBEF and TCL rank results based on multimodal encoders, while models such as CLIP rank using unimodal embedding similarity [25]. Fused models retrieve Top-N candidates for final ranking via a multimodal encoder.

Image Captioning (IC) [2, 33] generates textual descriptions of visual content, translating images into coherent captions. Unlike ITR, IC focuses on describing visual input, often evaluated using metrics like BLEU and CIDEr.

Visual Grounding (VG) [10, 16, 30] focuses on localizing objects or regions in an image based on text descriptions.

2.3 Universal Adversarial Perturbation

Research on the adversarial robustness of VLP models has gained significant attention, with prior studies [13, 28, 39] predominantly focusing on unimodality perturbations, thus limiting focus on cross-modal interactions.

To overcome this, Co-Attack [43] introduces a multimodal adversarial attack for VLP models, targeting image-text interactions to disrupt embedding distances between adversarial examples and original data pairs. It is applicable to models like CLIP, ALBEF, and TCL. SGA [20] enhances transferability by using set-level augmentations and cross-modal guidance, increasing data diversity and reducing similarity between adversarial examples and their matched modality. However, it remains instance-specific and limited in real-time applications. TMM [34] improves on SGA by better leveraging cross-modal interactions through optimizing modality-consistency and modality-discrepancy features.

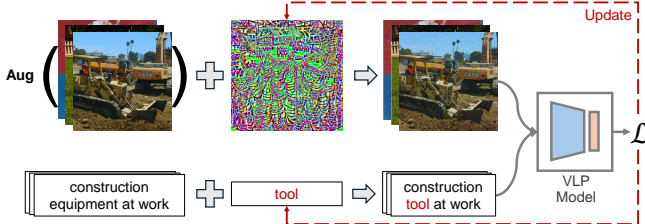


Figure 2: Pipeline of DO-UAP method.

To improve the applicability and generalizability in practice, several works have explored UAP for VLP models. Zhang et al. [44] proposed a pseudo-universal attack by applying UAP solely to the image modality, which does not constitute a truly universal attack for multimodal VLP models. In contrast, CPGC [8] introduced the first fully universal attack for VLP models by adding perturbations to both image and text modalities. Through contrastive training, the generator disrupts the alignment between image-text pairs, enhancing attack effectiveness across various vision-language tasks and models. However, their method involves optimizing a generator for UAP generation, which is time-consuming and unstable. To address this, we propose a more efficient UAP generation method using direct optimization.

3 Methodology

In this section, we begin by outlining the problem of universal adversarial attacks on VLP models, followed by a detailed introduction to our direct optimization method for UAP generation.

3.1 Problem Statement

3.1.1 Problem Definition. Let (v, t) represent an image-text pair from a multimodal dataset \mathcal{D} . The image encoder $f_I(\cdot)$ and text encoder $f_T(\cdot)$ are components of a target VLP model $f(\cdot)$. The objective of multimodal universal adversarial attacks is to generate **fixed** image-text perturbations (δ_v, δ_t) that can be applied universally across a large subset of (v, t) pairs from the test dataset \mathcal{D}_{test} , misleading the VLP model $f(\cdot)$ into making incorrect decisions.

3.1.2 Preliminary. The multimodal perturbations (δ_v, δ_t) are typically constrained to small magnitudes (ϵ_v, ϵ_t) . For the image modality, we follow the settings of prior work [8, 34] and adopt the strength ϵ_v of δ_v to be the value of 12/255 using the l_∞ norm. For the text modality, we adopt the setting of the previous work [8, 20, 34, 43], where key tokens in the original text t are replaced with crafted adversarial tokens. The textual perturbation is thus token-level, with ϵ_t restricted to substituting only one token per sentence (i.e., $\epsilon_t = 1$).

3.2 Method Design Intuition

Based on the empirical finding that generator-based attacks [24] surpass direct optimization-based attacks [21] in compromising VLP models, CPGC [8] proposes a generator-based UAP method specifically targeting VLP models. While this choice makes them easily achieve high attack performance, *they overlook a key drawback of generative methods: optimizing a generator for UAP generation is an*

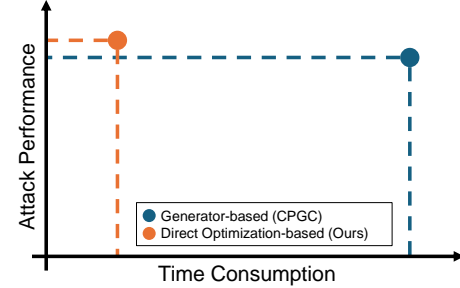


Figure 3: Compared to existing generator-based UAP methods, our proposed direct optimization-based UAP approach not only delivers higher attack performance but also significantly reduces time consumption.

indirect, time-consuming process. In contrast, directly optimizing the UAP with respect to the loss function is a more efficient and resource-saving solution (see Figure 3).

To develop a direct optimization-based method for universal adversarial attacks, an intuitive idea is to adopt the objective design utilized in previous universal adversarial attack methods [12, 24, 27] aimed at unimodality tasks, *i.e.*, maximizing the task-specific loss. Note that for clarity and conciseness, we use the image classification task as a representative example of an unimodality task. Specifically, in traditional image classification, the adversarial objective typically involves maximizing the cross-entropy loss between the model's prediction label and the ground truth label.

Similarly, for universal adversarial attacks targeting VLP models, as the V+L tasks (e.g., image-text retrieval, image captioning, visual grounding) are all cross-modal tasks that rely on the alignment between image and text, the basic objective is to maximize the loss $\mathcal{L}_t = \mathcal{J}(f_I(v'), f_T(t'))$ to disrupts the image-text alignment:

$$\max \mathcal{L}_t, \text{ s.t. } v' \in B[v, \epsilon_v], t' \in B[t, \epsilon_t], \quad (1)$$

where $v' = v + \delta_v$ representing the adversarial image and $t' = t \oplus \delta_t$ denoting adversarial text (\oplus means replace token). $\mathcal{J}(\cdot)$ is the training loss used in the VLP models. The allowable perturbations of (v, t) are restricted within the ranges $B[v, \epsilon_v]$ for images and $B[t, \epsilon_t]$ for text.

Method Overview. Following Eq.(1), the generated UAP demonstrates some level of attack effectiveness. However, the “modality gap” phenomenon in VLP is not fully considered, limiting the comprehensiveness of the attack. To this end, we propose a multimodal-oriented loss design in Sec. 3.3. Furthermore, to further boost the attack performance of our UAP method, we propose an idea for selecting a suitable data augmentation method, identifying brightness augmentation as a particularly effective choice, as detailed in Sec. 3.4. The pipeline of our DO-UAP method is in Figure 2. Given the image-text pairs, we first perform data augmentation on a batch of images for the image modality. Adversarial images are generated by adding UAP to these augmented images. For the text modality, key tokens in the original text are replaced with adversarial tokens. Both adversarial images and texts are then fed into the VLP model to compute the loss. This loss is subsequently used to update the UAP for both image and text modalities.

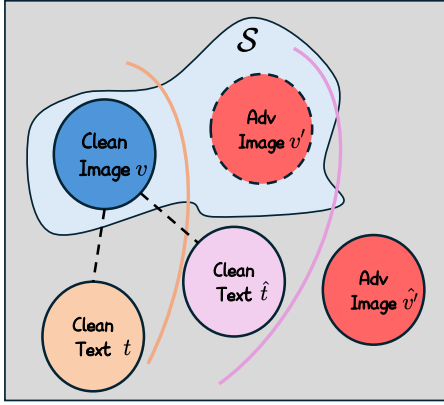


Figure 4: Motivation for multimodal loss design.

3.3 Multimodal-Oriented Loss Design

Given that the purpose of VLP models is to align image-text pairs, it is logical to design a cross-modal objective for universal adversarial attacks. However, the Eq. (1) is inadequate when accounting for the complexities of multimodal models. The complexity arises from the “modality gap” phenomenon in VLP models [17], where the embedding vectors of images and text are distinctly separated within the joint vision-language embedding space, as observed in VLP models like CLIP. If there is no “modality gap” phenomenon, the cross-modal objective is good enough.

To be specific, we give an explanation in Figure 4 to demonstrate the problem in Eq. (1) raised by this phenomenon. For simplicity and clarity, we focus solely on the UAP for image (*i.e.*, δ_v) though a similar reasoning applies to the text modality. In Figure 4, the image-text pair (v, t) from the original training dataset are in blue and orange circles respectively. In the image domain, the space \mathcal{S} represents the set of images with semantics similar to image v . The orange line indicates the semantic boundary, determining whether the semantics of an image align closely with the clean text t . When optimizing for a cross-modal objective, the semantics of the generated adversarial image v' (*i.e.*, $v + \delta_v$) diverge significantly from the text t (on both sides of the orange boundary), but may still reside within the space \mathcal{S} (represented by the red circle with a dotted outline). As the adversarial image v' retains similar semantics to the original image v , in comparison to other texts in the test dataset (*e.g.*, \hat{t} , represented by the purple circle) which correspond to the clean image v but differ semantically from t (purple vs. orange boundary), the VLP model is likely to retain the alignment of the adversarial image v' with \hat{t} . This results in poor attack performance of UAP δ_v generated solely based on the cross-modal objective.

To address the problem and enhance the attack performance of the UAP δ_v , we propose to add an unimodal objective. As shown in Figure 4, adding an unimodal objective into the clean image can push the adversarial image further away from the space \mathcal{S} , transforming it to be \hat{v}' (see a red circle with solid outline). Since adversarial image \hat{v}' is positioned outside space \mathcal{S} , there is a high probability that the image \hat{v}' and text \hat{t} are not aligned.

To summarize, we propose the necessary of a multimodal objective combining cross-modal loss and unimodal loss, expanding the

basic objective Eq. (1) to:

$$\mathcal{L}_u = \mathcal{D}(f_I(v'), f_I(v)) + \mathcal{D}(f_I(t'), f_I(t)) \quad (2)$$

$$\mathcal{L} = \mathcal{L}_t + \alpha \mathcal{L}_u \quad (3)$$

$$\max \mathcal{L}, \text{ s.t. } v' \in B[v, \epsilon_v], t' \in B[t, \epsilon_t], \quad (4)$$

where function $\mathcal{D}(\cdot)$ is used to evaluate the distance between embeddings and we use cosine similarity here. α is the weight.

3.4 Data Augmentation Selection

To further enhance the performance of UAP attacks, we leverage data augmentation, a well-established technique in deep learning [26, 36, 46]. The impact of data augmentation on UAP attacks specifically targeting VLP models has not yet been explored. Given that not all types of data augmentation are beneficial [6, 29], we aim to find an effective data augmentation for UAP generation.

Our high-level idea stems from analyzing the attack objective on VLP models (*i.e.*, Eq. (1)), where the goal of adversarial perturbation is designed to disrupt the alignment between text and image pairs. Let’s consider a special case where **misaligned image-text pairs** (*i.e.*, with low image-text similarity, such as an image of a dog paired with a text description of a computer) are used as input, instead of the typically aligned pairs (*i.e.*, with high image-text similarity, such as an image of a dog paired with a text description of a dog). Intuitively, when misaligned image-text pairs are used for UAP generation, their inherent misalignment already satisfies the attack objective and does not need UAP. As a result, the gradients calculated by such misaligned image-text pairs become less informative and meaningless for the UAP generation. Building on this insight, we suppose that data augmentations that enhance the similarity between image-text pairs can positively impact UAP generation. To this end, we conduct an empirical study on five data augmentation types (*i.e.*, compression, noise, flip, crop, and brightness) and try to find one that is effective for UAP generation. Note that in this study, we select these five types of data augmentation due to their widespread use in a variety of tasks. However, this choice does not imply that other augmentation techniques are unsuitable for generating UAPs. Additionally, our objective is not to exhaustively identify all effective data augmentation methods for UAP generation.

To evaluate the influence of data augmentations on image-text similarity, we apply them to the test dataset of Flickr30K [23] targeting CLIPViT model. The results are shown in Table 1. In the first row are the names of data augmentations and “origin” means no augmentation. In the “image-text similarity” row, we give the average value of image-text similarity in the test dataset of Flickr30K by calculating the cosine similarity of the image-text pair (v, t) , *i.e.*, $\text{CosineSim}(f_I(v), f_T(t))$. From the table, we can find that only the “brightness” augmentation can improve the image-text similarity while other augmentation methods (*e.g.*, “flip”) are not effective, or even reduce the similarity (*e.g.*, “compression”).

We further generate the UAP by attacking the CLIPViT model on the Flickr30K dataset with these data augmentation methods based on Eq. (3) and evaluate the performance of the generated UAP on the image-to-text retrieval (ITR) task. Note that for the ITR task, there are actually two tasks, image retrieval (IR) and text retrieval (TR). We report the average attack performance across both tasks in Table 1. The evaluation metric employed is the attack

Table 1: Evaluating the impact of various data augmentations on image-text similarity and the attack performance of UAP.

	Origin	Compression	Noise	Flip	Crop	Brightness
Image-text similarity	0.4562	0.4554	0.4554	0.4562	0.4484	0.4608
Attack performance \uparrow	92.765	89.155	88.125	92.640	90.210	94.360

Algorithm 1: DO-UAP Algorithm

```

Input: Training dataset  $\mathcal{D}$ , Loss  $\mathcal{L}$ , Batch size  $m$ , Number of epochs  $E$ , Perturbation magnitude  $\epsilon_v$  and  $\epsilon_t$ 
Output: Perturbation  $\delta_v$  and  $\delta_t$ 
1  $\delta_v, \delta_t \leftarrow 0$ ; ▷ initialization
2 for epoch = 1 to  $E$  do
3    $I \leftarrow |\mathcal{D}|/m$ ; ▷ iteration number
4   for iteration = 1 to  $I$  do
5      $\mathcal{P} \sim \mathcal{D} : |\mathcal{P}| = m$ ; ▷ randomly sample
6      $\mathcal{P} \leftarrow \text{Aug}(\mathcal{P})$ ; ▷ brightness augmentation
7      $g(\delta_v, \delta_t) \leftarrow \mathbb{E}_{(v, t) \sim \mathcal{P}} [\nabla_{(\delta_v, \delta_t)} \mathcal{L}]$ ; ▷  $\mathcal{L}$  from Eq. (3)
8      $\delta_v, \delta_t \leftarrow \text{Optim}(g(\delta_v, \delta_t))$ ; ▷ update UAP
9     let  $v + \delta_v \in B[v, \epsilon_v]$ ,  $t \oplus \delta_t \in B[t, \epsilon_t]$ ; ▷ clipping

```

success rate (ASR) on Recall@1 (R@1). R@1 is a standard metric in Image-Text Retrieval (ITR) tasks, where a score of 1 is assigned if the system retrieves a relevant result in the first position for a given query, and 0 otherwise. For UAP, a higher ASR indicates better performance. In the “attack performance” row of Table 1, we observe that only the UAP generated with “brightness” augmentation outperforms the version without augmentation. Augmentations that reduce image-text similarity result in worse attack performance of their corresponding UAP.

In summary, from the empirical study, we suggest adding brightness augmentation to the UAP generation algorithm. We also observe a positive correlation between the effect of data augmentation on image-text similarity and its impact on UAP performance. It is important to note that this phenomenon is observed with only certain types of data augmentation and may not be effective across all augmentation methods. As our primary objective is to identify a suitable augmentation for UAP generation, we did not pursue further exploration in this direction. However, we believe this is an interesting avenue for future research.

3.5 Implementation

Our proposed approach DO-UAP is implemented following Algorithm 1. In line 1, the UAP pair δ_v, δ_t are initialized. In line 2, executes the adversarial attack over E epochs. In line 3, the number of iterations I is determined. In line 4, carries out the adversarial attack iteratively for I iterations. In line 5, a random sample of training data \mathcal{P} is selected with a fixed batch size m . In line 6, apply brightness augmentation to data. In line 7, the gradient $g(\delta_v, \delta_t)$ for the UAP is calculated. In line 8, update the UAP pair (δ_v, δ_t) . In line 9, clipping the UAP (δ_v, δ_t) to satisfy the constraint.

4 Experiment

4.1 Experimental Setup

Downstream tasks and datasets. We conducted a comprehensive study of our method across three downstream V+L tasks, namely image-text retrieval (ITR), image captioning (IC), and visual grounding (VG). The datasets used for these tasks are as follows:

- The Flickr30K dataset [23], sourced from the Flickr website, provides detailed descriptions of objects and activities, making it a widely used benchmark for various V+L tasks. It comprises 31,783 images, each accompanied by five captions. We utilize this dataset for ITR tasks.
- The MSCOCO dataset [19] is a comprehensive and diverse collection containing 123,287 images, each annotated with approximately five descriptive sentences. This dataset is employed to assess attack performance in both ITR and IC tasks.
- The RefCOCO+ dataset [41], a subset of MSCOCO, includes 19,992 images and 141,564 annotations, specifically designed for VG tasks.

Surrogate models and victim models. For the ITR tasks, we employ CLIPViT, CLIPCNN [25], BLIP [14] ALBEF [15], TCL [40], and X-VLM [42], as victim models. Notably, different image feature extraction modules are used for CLIP: ViT-B/16 for CLIPViT and ResNet-101 for CLIPCNN, while the other models rely solely on ViT for image feature extraction. For the VG tasks, ALBEF, TCL, and X-VLM serve as both surrogate and victim models. For the IC tasks, BLIP is used as the victim model. Notably, out of the six VLP models, only ALBEF, TCL, and X-VLM can handle VG tasks, while only BLIP is capable of managing IC tasks.

Metrics. We use the attack success rate (ASR) as the primary metric to assess the effectiveness of our universal adversarial samples. ASR measures the extent to which adversarial perturbations cause deviations from correct decisions in the victim models. In ITR tasks, metrics such as R@1, R@5, and R@10 are typically used to calculate ASR, where R@N denotes the top N most relevant text or image matches based on a query. Due to space constraints, we only report the ASR for R@1 in our main results. For other cross-modal downstream V+L tasks, including IC and VG, their respective evaluation metrics will be outlined when presenting the experimental results in subsequent sections.

Baselines. We adopt the widely recognized and powerful GAP algorithm [24] to the multimodal attack scenario by modifying its original loss function. Additionally, we compare our method with state-of-the-art (SOTA) methods CPGC [8].

Implementation details. In line with prior works [8], we utilize the Karpathy split [22] to preprocess the dataset and construct the test set for performance evaluation. Also, following [8], for Flickr30K and MSCOCO, we randomly select 30,000 images along with their corresponding captions from the training set. For SNLI-VE and RefCOCO+, we directly utilize their respective training sets, consisting of 29,783 and 16,992 images. Regarding the perturbation budget, we follow the setting of previous work [8, 34], constraining the visual perturbation ϵ_v to 12/255 and limiting the language perturbation ϵ_t to 1 to maintain invisibility. We set the number of training epochs for our DO-UAP to 2, using the brightness data augmentation range of [0, 0.05]. For the parameter α in Eq. (3), which balances the cross-modal and unimodal losses, we set $\alpha = 1$. For

Table 2: Compare with baselines.

Dataset	Methods	CLIP _{ViT}		CLIP _{CNN}		BLIP		TCL		X-VLM		ALBEF		Average		Time (hours)
		TR	IR	TR	IR	TR	IR	TR	IR	TR	IR	TR	IR	TR	IR	
Flickr30K	GAP	81.63	83.91	76.11	85.20	48.16	73.70	84.20	80.34	80.35	76.91	72.46	82.69	73.82	80.46	5.22
	CPGC-2	91.13	93.75	80.18	87.15	69.93	78.49	91.72	87.46	81.81	82.19	87.67	84.92	83.74	85.66	6.71
	CPGC-40	89.04	93.59	82.12	88.94	80.63	87.31	95.45	91.57	93.70	92.20	90.24	89.51	88.53	90.52	134.19
	DO-UAP (ours)	93.35	95.37	93.13	93.84	88.33	91.98	94.10	91.36	97.36	94.55	94.45	93.55	93.45	93.44	5.83
MSCOCO	GAP	97.79	96.38	91.43	94.47	75.17	73.76	95.66	92.98	95.47	89.53	83.63	84.82	89.86	88.66	5.21
	CPGC-2	96.07	96.91	95.06	95.09	88.14	86.36	94.31	87.60	96.65	92.01	85.87	83.58	92.68	90.26	6.51
	CPGC-40	98.97	98.14	95.30	94.59	95.84	95.86	97.20	94.35	99.04	96.07	96.49	95.47	97.14	95.75	130.13
	DO-UAP (ours)	98.13	98.01	96.90	98.01	88.38	87.31	98.73	96.51	98.23	96.02	96.73	97.23	96.18	95.52	5.63

the attack strength per iteration, we set it to 0.1 of the perturbation budget. All the experiments are run on a Ubuntu system with an NVIDIA A100 Tensor of 80G RAM.

4.2 Compare with SOTA Baseline

In alignment with previous adversarial attacks on VLP models [8, 20, 43], our focus is on the multimodal task of image-text retrieval, rather than image captioning or visual grounding tasks. This encompasses both image retrieval (IR) and text retrieval (TR). We conduct extensive experiments on the Flickr30K and MSCOCO datasets to assess the attack efficacy of the proposed DO-UAP. The experimental results across six different VLP models are summarized in Table 2. We report the attack success rate (higher is better) on R@1 (results on R@5 and R@10 are in Appendix A.1). We introduce a comparison with the basic generator-based UAP methods GAP [24] and the state-of-the-art UAP method CPGC [8]. In Table 2, it is important to note that while CPGC optimizes its generator over 40 epochs (“CPGC-40” row) in the original work, our DO-UAP method requires only 2 epochs, resulting in considerable time savings. For a fair comparison, we also limit CPGC to 2 epochs, with the results presented in the “CPGC-2” row. We also tracked the time consumption and present the average values here, with detailed records provided in Section 4.3.

Regarding the Flickr30K dataset, our method surpasses CPGC-40, achieving an average improvement of 4.92% on the TR task and 2.92% on the IR task across six models. Additionally, it significantly outperforms CPGC-2 and GAP by nearly 10%. Notably, our DO-UAP method completes UAP generation in just 5.83 hours, significantly faster than the time-consuming CPGC-40, which takes an average of 134.19 hours across the same six models, representing a time efficiency improvement of approximately 23-fold.

Regarding the MSCOCO dataset, our method performs comparably to CPGC-40, with a slight average decrease of 0.96% in the TR task and 0.23% in the IR task across six models. However, it significantly surpasses CPGC-2 and GAP by nearly 5%. Notably, our method generates UAP in just 5.63 hours, significantly faster than the 130.13 hours required by CPGC-40 across the same six models, representing a roughly 23-fold improvement in time efficiency.

In summary, across both Flickr30K and MSCOCO datasets, our DO-UAP method surpasses CPGC in attack performance, with an improvement of 1.98% on the TR task and 1.33% on the IR task. More importantly, our DO-UAP method is stably more efficient than

Table 3: Comparison of time consumption.

Dataset	Methods	CLIP _{ViT}	CLIP _{CNN}	BLIP	TCL	X-VLM	ALBEF
Flickr30K	GAP	2.86	2.14	6.50	6.14	7.78	5.92
	CPGC-2	4.06	3.54	9.56	7.58	7.84	7.68
	CPGC-40	81.20	70.80	191.20	151.60	156.80	153.52
	DO-UAP (ours)	3.80	2.94	6.94	7.22	7.24	6.84
MSCOCO	GAP	2.84	2.12	6.20	6.52	7.80	5.78
	CPGC-2	3.82	3.52	8.94	7.42	7.84	7.50
	CPGC-40	76.40	70.40	178.80	148.40	156.80	150.00
	DO-UAP (ours)	3.60	2.66	6.80	6.92	7.10	6.68

CPGC, being 20 times faster. Specifically, our method generates UAP in just six hours, while CPGC requires over five days.

4.3 Time Consumption

For a detailed understanding of the efficiency of our DO-UAP method, we list the detailed time consumption across six VLP models on the Flickr30K and MSCOCO datasets. As shown in Table 3, the time units for the data are in hours. Across six models, all the methods perform faster on CLIP_{ViT} and CLIP_{CNN}, while being slower on the other four models. Compared to CPGC-40 (40 epochs), our DO-UAP method is significantly faster overall. Even with the same number of epochs as CPGC-2 (2 epochs), our method demonstrates a slight speed advantage.

4.4 Visualization

We visualize the UAPs generated by our DO-UAP method and their effect on the ITR, IC, and VG tasks as an example in Figure 5, Figure 6, and Figure 7. In Figure 5(a), given the adversarial query image, we present the ground-truth text alongside the retrieved top-5 texts. It is evident that the retrieved texts differ significantly from the semantics of the query image. Also in Figure 5(b), for a given adversarial query text, the top-5 retrieved images are all inconsistent with the query. In Figure 6, the VLP model (BLIP) generates a text caption with a meaning that deviates from the actual content of the adversarial image. In Figure 7, when provided with a text caption and key word, the model is able to correctly identify and locate the “boy” in the clean image but fails to do so in the adversarial image.

4.5 Ablation Study

4.5.1 Multimodal loss design. For the parameter α in Eq. (3) which balances the cross-modal and unimodal losses, we conducted an

 <p>Query</p>	<p>Ground-truth texts</p> <ol style="list-style-type: none"> 1. 'the man with pierced ears is wearing glasses and an orange hat' 2. 'a man with glasses is wearing a beer can crocheted hat' 3. 'a man with gauges and glasses is wearing a blitz hat' 4. 'a man in an orange hat staring at something' 5. 'a man wears an orange hat and glasses'
	<p>Retrieved top-5 texts</p> <ol style="list-style-type: none"> 1. 'a biennial waring a polo shirt fixes a ticket machine while per-sons line up at an adjoining machine' 2. 'a man in a chefs uniform biennial a large skillet over a stove with fire coming out of the skillet' 3. 'his eyes filled with joyous expectation a biennial prepares for a jump' 4. 'a japanese man biennial a flute from sheet music beside a tree lines river' 5. 'there is a biennial by a body of water a man bicycles by'

(a) Image-to-Text retrieval

 <p>Query:</p> <p>'a man with gauges and glasses is wearing a biennial (blitz) hat'</p>	<p>Ground-truth</p>	<p>Retrieved top-5 images</p> 
	<p>Query:</p> <p>'a photographer takes a picture of a group of one girl in a biennial (pink) dress and 10 boys in suits and hats'</p>	<p>Ground-truth</p>

(b) Text-to-Image retrieval

Figure 5: Visualization of image-text retrieval task.

 <p>Query</p>	<p>Ground-truth texts</p> <ol style="list-style-type: none"> 1. 'a kitchen is shown with a variety of items on the counters' 2. 'a kitchen has the windows open and plaid curtains' 3. 'a kitchen with two windows and two metal sinks' 4. 'an older kitchen with cluttered counter tops but empty sink' 5. 'glasses and bottles are placed near a kitchen sink'
	<p>BLIP generated texts</p> <p>'a book with a picture of a man in a suit and tie'</p>

Figure 6: Visualization of image caption task.



Figure 7: Visualization of visual grounding task.

Table 4: Ablation on weight of unimodal loss.

α	0	0.1	1	10
TR	87.68	89.04	91.75	91.63
IR	91.90	93.94	93.81	92.28
Average	89.79	91.49	92.78	91.95

Table 5: Ablation on brightness augmentation.

Brightness	N/A	[0, 0.05]	[0, 0.10]	[0, 0.15]	[0, 0.20]
TR	91.75	93.35	90.27	89.29	88.67
IR	93.81	95.37	92.89	92.25	93.24
Average	92.78	94.36	91.58	90.77	90.96
Image-text Similarity	0.4562	0.4608	0.4525	0.4550	0.4444

ablation study. The results presented do not include data augmentation, to identify the influence of the unimodal loss.

Table 6: Ablation of perturbation magnitude per iteration.

β	0.1	0.3	0.5	0.7	0.9
TR	93.35	91.38	87.68	80.79	68.84
IR	95.37	94.80	94.29	82.07	76.94
Average	94.36	93.09	90.98	81.43	72.89

Table 7: Ablation study of attack strength.

Attack strength	4/255	8/255	12/255	16/255
TR	56.53	81.40	93.35	96.92
IR	65.36	90.33	95.37	97.38

As shown in Table 4, the values of α are in the first row. We report the attack success rates for TR (second row) and IR (third row), followed by the average (fourth row). It is evident that when α is set to zero (i.e., without the unimodal loss), the attack performance of UAP is the lowest, underscoring the importance of the unimodal loss. Furthermore, we observe that when α is set to one, the average attack performance is maximized. Therefore, we select $\alpha = 1$ in the final version of our method.

4.5.2 Data augmentation. Based on the multimodal objective Eq. (4), we conducted an ablation study to evaluate the impact of brightness augmentation at varying levels of severity. The results highlight the specific influence of this augmentation on attack performance.

As shown in Table 5, the first row lists the brightness values, representing the range of brightness enhancement applied. We report the attack success rates for TR (second row) and IR (third row), followed by the average (fourth row). It is evident that when the brightness range is [0, 0.05], the attack performance of UAP improves for both TR and IR, with an increase of approximately 2%. However, excessive augmentation severity does not enhance attack performance. Regarding image-text similarity, only brightness within the range [0, 0.05] leads to an improvement, which aligns with the observed boost in attack performance. This indicates that

Table 8: Performance on cross data.

Train Dataset	Test Dataset	CLIPViT		CLIPCNN		BLIP		TCL		X-VLM		ALBEF		Average	
		TR	IR	TR	IR	TR	IR	TR	IR	TR	IR	TR	IR	TR	IR
Flickr30K	MSCOCO	96.68	96.65	97.67	97.04	93.63	92.98	97.09	94.61	97.83	94.54	97.86	96.32	96.79	95.36
MSCOCO	Flickr30K	92.49	95.12	92.62	95.34	66.77	72.92	95.55	91.57	82.42	83.01	87.36	91.34	86.20	88.22

Table 9: Performance on image captioning.

	B@4 ↓	METEOR ↓	ROUBE_L ↓	CIDEr ↓	SPICE ↓
BLIP (No attack)	39.7	31.0	60.0	133.3	23.8
BLIP (Attack)	24.3	23.3	48.0	82.4	16.3

Table 10: Performance on visual grounding.

Source	Target	Val	TestA	TestB
ALBEF (No attack)	ALBEF	58.4	65.9	46.2
ALBEF (Attack)		40.7	45.8	34.1
TCL (Attack)		53.3	59.2	43.1
X-VLM (Attack)		56.7	62.7	44.4
TCL (No attack)	TCL	59.6	66.8	48.1
ALBEF (Attack)		56.7	63.5	46.1
TCL (Attack)		49.6	54.7	40.4
X-VLM (Attack)		58.2	64.8	46.8
X-VLM (No attack)	X-VLM	70.8	78.2	62.5
ALBEF (Attack)		65.2	69.7	58.0
TCL (Attack)		65.1	70.2	57.9
X-VLM (Attack)		65.1	69.7	57.3

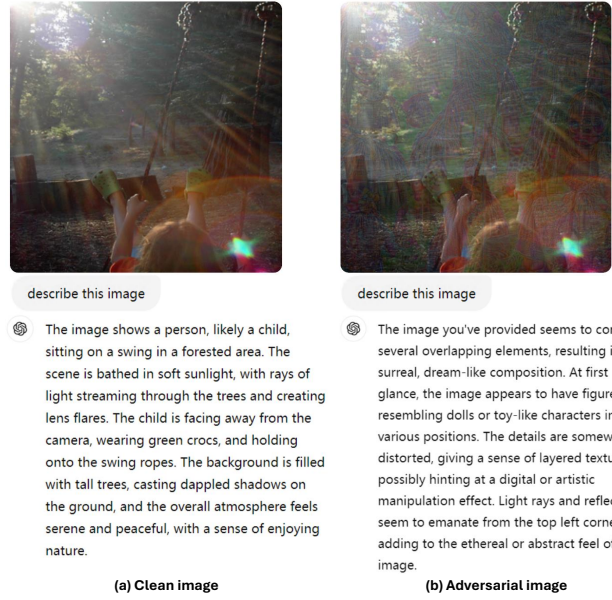
brightness augmentation, when it improves image-text similarity, also enhances attack effectiveness. Based on the ablation, we select [0, 0.05] brightness in the final version of our method.

4.5.3 Attack strength per iteration. Based on the DO-UAP method, we conducted an ablation study to evaluate the impact of perturbation magnitude per iteration (β). The results reflect the significant influence of β on attack performance.

As shown in Table 6, the first row lists the magnitude values, representing the magnitude value in each iteration accounting for how much of the total strength (ϵ_v, ϵ_t). We report the attack success rates for TR (second row) and IR (third row), followed by the average (fourth row). It is clear that when β is set to 0.1, the attack performance of UAP is optimal. Higher values of β lead to a decline in performance. Therefore, we select $\beta = 0.1$ in the final version of our method.

4.5.4 Attack strength. The magnitude of image perturbations serves as a critical metric for evaluating adversarial attacks. As demonstrated in Table 7, we assessed the attack performance across different perturbation levels, varying from 4/255 to 16/255.

Overall, the attack performance improves as the perturbation magnitude increases. At a perturbation magnitude of 4/255, the performance is notably constrained. This is because, with a limited

**Figure 8: Effect on LViM ChatGPT 4o.**

budget of 4/255, a single common perturbation lacks sufficient capacity to generalize across diverse data samples. Furthermore, from 12/255 to 16/255, the rate of improvement begins to plateau as the perturbation budget grows.

4.6 Evaluation on More Scenarios

To further demonstrate the effectiveness of the proposed DO-UAP algorithm, we evaluate its performance in various scenarios, including additional downstream vision-and-language (V+L) tasks, cross-domain transfer, and attacks on state-of-the-art large vision-language models (LVLMs).

4.6.1 IC. Image captioning aims to encode an input image into embeddings, which are then used by an image-conditioned language model to generate text descriptions relevant to the image's content. In this work, we utilize BLIP as the victim model, focusing on directly attacking it using the MSCOCO dataset. Following CPGC [8], we calculate several standard metrics to assess the quality of the generated captions, including BLEU [22], METEOR [3], ROUGE [18], CIDEr [32], and SPICE [1]. All these metrics are lower is better for the attack task. Table 9 demonstrates that our DO-UAP method exhibits significant attack effects on the image captioning task.

4.6.2 VG. Visual grounding is a widely studied vision-and-language (V+L) task that focuses on identifying the correct location in an image based on a given textual description. We perform experiments on the RefCOCO+ dataset, using ALBEF, TCL, and X-VLM as both source and target models. As shown in Table 10, we report the accuracy (lower is better) for each dataset Val, TestA, and TestB. The results demonstrate that our attack effectively reduces localization accuracy, further confirming that the generated UAP effectively disrupts cross-modal interaction and alignment.

4.6.3 Cross data. We evaluate the attack performance of the proposed DO-UAP method in a more challenging scenario involving a clear distribution shift between the training and testing data. Specifically, we generate UAP using either the MSCOCO or Flickr30K dataset and assess their transferability to the other. The ASRs are presented in Table 8. We can find the UAP generated by our method has strong transferability across different data domains.

4.6.4 Transfer to LVLMs. Recently, large general models capable of handling complex vision-language tasks have garnered widespread attention. To further illustrate the potential threat of our method in practical scenarios, *i.e.*, online applications, we aim to evaluate the performance of DO-UAP on mainstream LVLMs ChatGPT 4.0. For example, in Figure 8, the adversarial image with UAP generated by X-VLM can mislead the ChatGPT 4.0.

5 Conclusion

In this paper, we propose a direct optimization-based UAP approach, termed DO-UAP, which significantly reduces resource consumption while maintaining high attack performance. Specifically, we investigate the necessity of multimodal loss design and introduce an efficient data augmentation strategy. In future work, we aim to enhance the transferability of our algorithm, making the method more practical in a black box setting.

References

- [1] Peter Anderson, Basura Fernando, Mark Johnson, and Stephen Gould. 2016. Spice: Semantic propositional image caption evaluation. In *Computer Vision–ECCV 2016: 14th European Conference, Amsterdam, The Netherlands, October 11–14, 2016, Proceedings, Part V 14*. Springer, 382–398.
- [2] Shuang Bai and Shan An. 2018. A survey on automatic image caption generation. *Neurocomputing* 311 (2018), 291–304.
- [3] Satanjeev Banerjee and Alon Lavie. 2005. METEOR: An automatic metric for MT evaluation with improved correlation with human judgments. In *Proceedings of the acl workshop on intrinsic and extrinsic evaluation measures for machine translation and/or summarization*. 65–72.
- [4] Min Cao, Shiping Li, Juntao Li, Liqiang Nie, and Min Zhang. 2022. Image-text Retrieval: A Survey on Recent Research and Development. In *Proceedings of the Thirty-First International Joint Conference on Artificial Intelligence, IJCAI-22*. International Joint Conferences on Artificial Intelligence Organization, 5410–5417. <https://doi.org/10.24963/ijcai.2022/759> Survey Track.
- [5] Fei-Long Chen, Du-Zhen Zhang, Ming-Lun Han, Xiu-Yi Chen, Jing Shi, Shuang Xu, and Bo Xu. 2023. Vlp: A survey on vision-language pre-training. *Machine Intelligence Research* 20, 1 (2023), 38–56.
- [6] Ekin Dogus Cubuk, Ethan S Dyer, Rapha Gontijo Lopes, and Sylvia Smullin. 2021. Tradeoffs in data augmentation: An empirical study. In *International Conference on Learning Representations (ICLR)*.
- [7] Alexey Dosovitskiy, Lucas Beyer, Alexander Kolesnikov, Dirk Weissenborn, Xiaohua Zhai, Thomas Unterthiner, Mostafa Dehghani, Matthias Minderer, Georg Heigold, Sylvain Gelly, Jakob Uszkoreit, and Neil Houlsby. 2021. An Image is Worth 16x16 Words: Transformers for Image Recognition at Scale. In *International Conference on Learning Representations*. <https://openreview.net/forum?id=YicbFdNTTy>
- [8] Hao Fang, Jiawei Kong, Wenbo Yu, Bin Chen, Jiawei Li, Shutao Xia, and Ke Xu. 2024. One Perturbation is Enough: On Generating Universal Adversarial Perturbations against Vision-Language Pre-training Models. *arXiv preprint arXiv:2406.05491* (2024).
- [9] Kai Han, Yunhe Wang, Hanting Chen, Xinghao Chen, Jianyuan Guo, Zhenhua Liu, Yehui Tang, An Xiao, Chunjing Xu, Yixing Xu, et al. 2022. A survey on vision transformer. *IEEE transactions on pattern analysis and machine intelligence* 45, 1 (2022), 87–110.
- [10] Richang Hong, Daqing Liu, Xiaoyu Mo, Xiangnan He, and Hanwang Zhang. 2022. Learning to Compose and Reason with Language Tree Structures for Visual Grounding. *IEEE Transactions on Pattern Analysis and Machine Intelligence* 44, 2 (2022), 684–696. <https://doi.org/10.1109/TPAMI.2019.2911066>
- [11] Xiaowei Hu, Zhe Gan, Jianfeng Wang, Zhengyuan Yang, Zicheng Liu, Yumao Lu, and Lijuan Wang. 2022. Scaling up vision-language pre-training for image captioning. In *Proceedings of the IEEE/CVF conference on computer vision and pattern recognition*. 17980–17989.
- [12] Yihao Huang, Qing Guo, Felix Juefei-Xu, Ming Hu, Xiaojun Jia, Xiaochun Cao, Geguang Pu, and Yang Liu. 2024. Texture Re-Scalable Universal Adversarial Perturbation. *Trans. Info. For. Sec.* 19 (June 2024), 8291–8305. <https://doi.org/10.1109/TIFS.2024.3416030>
- [13] Taewan Kim and Joydeep Ghosh. 2019. On single source robustness in deep fusion models. *Advances in Neural Information Processing Systems* 32 (2019).
- [14] Junnan Li, Dongxu Li, Caiming Xiong, and Steven Hoi. 2022. BLIP: Bootstrapping Language-Image Pre-training for Unified Vision-Language Understanding and Generation. In *International Conference on Machine Learning, ICML 2022, 17–23 July 2022, Baltimore, Maryland, USA (Proceedings of Machine Learning Research, Vol. 162)*. PMLR, 12888–12900.
- [15] Junnan Li, Ramprasaath Selvaraju, Akhilesh Gotmare, Shafiq Joty, Caiming Xiong, and Steven Chu Hong Hoi. 2021. Align before fuse: Vision and language representation learning with momentum distillation. *Advances in neural information processing systems* 34 (2021), 9694–9705.
- [16] Yunzhu Li, Toru Lin, Kexin Yi, Daniel Bear, Daniel Yamins, Jiajun Wu, Joshua Tenenbaum, and Antonio Torralba. 2020. Visual grounding of learned physical models. In *International conference on machine learning*. PMLR, 5927–5936.
- [17] Victor Weixin Liang, Yuhui Zhang, Yongchan Kwon, Serena Yeung, and James Y Zou. 2022. Mind the gap: Understanding the modality gap in multi-modal contrastive representation learning. *Advances in Neural Information Processing Systems* 35 (2022), 17612–17625.
- [18] Chin-Yew Lin. 2004. Rouge: A package for automatic evaluation of summaries. In *Text summarization branches out*. 74–81.
- [19] Tsung-Yi Lin, Michael Maire, Serge Belongie, James Hays, Pietro Perona, Deva Ramanan, Piotr Dollár, and C Lawrence Zitnick. 2014. Microsoft coco: Common objects in context. In *Computer Vision–ECCV 2014: 13th European Conference, Zurich, Switzerland, September 6–12, 2014, Proceedings, Part V 13*. Springer, 740–755.
- [20] Dong Lu, Zhiqiang Wang, Teng Wang, Weili Guan, Hongchang Gao, and Feng Zheng. 2023. Set-level guidance attack: Boosting adversarial transferability of vision-language pre-training models. In *Proceedings of the IEEE/CVF International Conference on Computer Vision*. 102–111.

- [21] Seyed-Mohsen Moosavi-Dezfooli, Alhussein Fawzi, Omar Fawzi, and Pascal Frossard. 2017. Universal adversarial perturbations. In *Proceedings of the IEEE conference on computer vision and pattern recognition*. 1765–1773.
- [22] Kishore Papineni, Salim Roukos, Todd Ward, and Wei-Jing Zhu. 2002. Bleu: a method for automatic evaluation of machine translation. In *Proceedings of the 40th annual meeting of the Association for Computational Linguistics*. 311–318.
- [23] Bryan A Plummer, Liwei Wang, Chris M Cervante, Juan C Caicedo, Julia Hockenmaier, and Svetlana Lazebnik. 2015. Flickr30k entities: Collecting region-to-phrase correspondences for richer image-to-sentence models. In *Proceedings of the IEEE international conference on computer vision*. 2641–2649.
- [24] Omid Poursaeed, Isay Katsman, Bicheng Gao, and Serge Belongie. 2018. Generative adversarial perturbations. In *Proceedings of the IEEE conference on computer vision and pattern recognition*. 4422–4431.
- [25] Alec Radford, Jong Wook Kim, Chris Hallacy, Aditya Ramesh, Gabriel Goh, Sandhini Agarwal, Girish Sastry, Amanda Askell, Pamela Mishkin, Jack Clark, et al. 2021. Learning transferable visual models from natural language supervision. In *International conference on machine learning*. PMLR, 8748–8763.
- [26] Sylvestre-Alvise Rebuffi, Sven Gowal, Dan Andrei Calian, Florian Stimberg, Olivia Wiles, and Timothy A Mann. 2021. Data augmentation can improve robustness. *Advances in Neural Information Processing Systems* 34 (2021), 29935–29948.
- [27] Ali Shafahi, Mahyar Najibi, Zheng Xu, John Dickerson, Larry S Davis, and Tom Goldstein. 2020. Universal adversarial training. In *Proceedings of the AAAI Conference on Artificial Intelligence*, Vol. 34. 5636–5643.
- [28] Meet Shah, Xinlei Chen, Marcus Rohrbach, and Devi Parikh. 2019. Cycle-consistency for robust visual question answering. In *Proceedings of the IEEE/CVF Conference on Computer Vision and Pattern Recognition*. 6649–6658.
- [29] Ruoqi Shen, Sébastien Bubeck, and Suriya Gunasekar. 2022. Data augmentation as feature manipulation. In *International conference on machine learning*. PMLR, 19773–19808.
- [30] Robik Shrestha, Kushal Kafle, and Christopher Kanan. 2020. A negative case analysis of visual grounding methods for VQA. In *Proceedings of the 58th Annual Meeting of the Association for Computational Linguistics*, Dan Jurafsky, Joyce Chai, Natalie Schluter, and Joel Tetreault (Eds.). Association for Computational Linguistics, Online, 8172–8181. <https://doi.org/10.18653/v1/2020.acl-main.727>
- [31] Haoyu Song, Li Dong, Weinan Zhang, Ting Liu, and Furu Wei. 2022. CLIP Models are Few-Shot Learners: Empirical Studies on VQA and Visual Entailment. In *Proceedings of the 60th Annual Meeting of the Association for Computational Linguistics (Volume 1: Long Papers)*. Association for Computational Linguistics, Dublin, Ireland, 6088–6100. <https://doi.org/10.18653/v1/2022.acl-long.421>
- [32] Ramakrishna Vedantam, C Lawrence Zitnick, and Devi Parikh. 2015. Cider: Consensus-based image description evaluation. In *Proceedings of the IEEE conference on computer vision and pattern recognition*. 4566–4575.
- [33] Oriol Vinyals, Alexander Toshev, Samy Bengio, and Dumitru Erhan. 2015. Show and tell: A neural image caption generator. In *Proceedings of the IEEE conference on computer vision and pattern recognition*. 3156–3164.
- [34] Haodi Wang, Kai Dong, Zhilei Zhu, Haotong Qin, Aishan Liu, Xiaolin Fang, Jiakai Wang, and Xianglong Liu. 2024. Transferable multimodal attack on vision-language pre-training models. In *2024 IEEE Symposium on Security and Privacy (SP)*. IEEE Computer Society, 102–102.
- [35] Kaiye Wang, Qiyue Yin, Wei Wang, Shu Wu, and Liang Wang. 2016. A comprehensive survey on cross-modal retrieval. *arXiv preprint arXiv:1607.06215* (2016).
- [36] Zaitian Wang, Pengfei Wang, Kunpeng Liu, Pengyang Wang, Yanjie Fu, Chang-Tien Lu, Charu C Aggarwal, Jian Pei, and Yuanchun Zhou. 2024. A Comprehensive Survey on Data Augmentation. *arXiv preprint arXiv:2405.09591* (2024).
- [37] Cihang Xie, Zhihuai Zhang, Yuyin Zhou, Song Bai, Jianyu Wang, Zhou Ren, and Alan L Yuille. 2019. Improving transferability of adversarial examples with input diversity. In *Proceedings of the IEEE/CVF conference on computer vision and pattern recognition*. 2730–2739.
- [38] Ning Xie, Farley Lai, Derek Doran, and Asim Kadav. 2019. Visual Entailment: A Novel Task for Fine-Grained Image Understanding. *ArXiv abs/1901.06706* (2019). <https://api.semanticscholar.org/CorpusID:58981654>
- [39] Xiaojun Xu, Xinyun Chen, Chang Liu, Anna Rohrbach, Trevor Darrell, and Dawn Song. 2018. Fooling vision and language models despite localization and attention mechanism. In *Proceedings of the IEEE Conference on Computer Vision and Pattern Recognition*. 4951–4961.
- [40] Jinyu Yang, Jiali Duan, Son Tran, Yi Xu, Sampath Chanda, Liqun Chen, Belinda Zeng, Trishul Chilimbi, and Junzhou Huang. 2022. Vision-Language Pre-Training with Triple Contrastive Learning. In *Proceedings of the IEEE conference on computer vision and pattern recognition*. IEEE, 15650–15659.
- [41] Licheng Yu, Patrick Poirson, Shan Yang, Alexander C Berg, and Tamara L Berg. 2016. Modeling context in referring expressions. In *Computer Vision–ECCV 2016: 14th European Conference, Amsterdam, The Netherlands, October 11–14, 2016, Proceedings, Part II* 14. Springer, 69–85.
- [42] Yan Zeng, Xinsong Zhang, and Hang Li. 2022. Multi-Grained Vision Language Pre-Training: Aligning Texts with Visual Concepts. In *Proceedings of the 39th International Conference on Machine Learning (Proceedings of Machine Learning Research, Vol. 162)*, Kamalika Chaudhuri, Stefanie Jegelka, Le Song, Csaba Szepesvari, Gang Niu, and Sivan Sabato (Eds.). PMLR, 25994–26009. <https://proceedings.mlr.press/v162/zeng22c.html>
- [43] Jiaming Zhang, Qi Yi, and Jitao Sang. 2022. Towards Adversarial Attack on Vision-Language Pre-training Models. In *Proceedings of the 30th ACM International Conference on Multimedia*. ACM, 5005–5013.
- [44] Peng-Fei Zhang, Zi Huang, and Guangdong Bai. 2024. Universal Adversarial Perturbations for Vision-Language Pre-trained Models. In *Proceedings of the 47th International ACM SIGIR Conference on Research and Development in Information Retrieval*. 862–871.
- [45] Qi Zhang, Zhen Lei, Zhaoxiang Zhang, and Stan Z Li. 2020. Context-aware attention network for image-text retrieval. In *Proceedings of the IEEE/CVF conference on computer vision and pattern recognition*. 3536–3545.
- [46] Zhun Zhong, Liang Zheng, Guoliang Kang, Shaizi Li, and Yi Yang. 2020. Random erasing data augmentation. In *Proceedings of the AAAI conference on artificial intelligence*, Vol. 34. 13001–13008.

Table 11: Compare with baselines (R@5).

Dataset	Methods	CLIP _{ViT}		CLIP _{CNN}		BLIP		TCL		X-VLM		ALBEF		Average		Time (hours)
		TR	IR	TR	IR	TR	IR	TR	IR	TR	IR	TR	IR	TR	IR	
Flickr30K	GAP	71.76	75.20	60.32	71.91	39.64	68.55	79.39	73.75	72.30	68.29	59.02	75.47	63.74	72.20	5.22
	CPGC-2	81.24	85.18	61.36	72.62	53.22	65.41	85.89	78.14	67.80	69.64	78.56	73.07	71.35	74.01	6.71
	CPGC-40	75.85	85.76	64.74	74.37	63.48	80.53	91.79	85.12	90.10	86.31	84.37	80.67	78.39	82.13	134.19
	DO-UAP (ours)	86.42	89.90	83.23	86.45	78.07	86.58	89.79	85.30	95.10	90.46	88.68	87.39	86.88	87.68	5.83
MSCOCO	GAP	95.37	93.40	89.02	90.12	64.68	68.31	93.06	88.45	91.47	83.76	75.51	79.39	84.85	83.91	5.21
	CPGC-2	92.78	93.76	90.32	90.42	79.66	79.70	89.15	77.57	92.79	85.09	77.17	75.40	86.98	83.66	6.51
	CPGC-40	96.76	96.57	91.95	89.34	92.46	93.40	95.24	91.04	96.95	91.93	93.78	91.98	94.52	92.38	130.13
	DO-UAP (ours)	95.45	95.54	93.94	96.35	80.77	81.21	97.39	93.89	96.68	93.13	93.30	95.36	92.92	92.58	5.63

Table 12: Compare with baselines (R@10).

Dataset	Methods	CLIP _{ViT}		CLIP _{CNN}		BLIP		TCL		X-VLM		ALBEF		Average		Time (hours)
		TR	IR	TR	IR	TR	IR	TR	IR	TR	IR	TR	IR	TR	IR	
Flickr30K	GAP	67.30	70.42	56.56	63.02	37.61	67.59	77.10	70.32	67.80	63.60	53.90	72.74	60.05	67.95	5.22
	CPGC-2	77.30	79.79	52.66	64.72	46.54	58.99	83.10	72.88	61.30	64.23	72.20	67.08	65.52	67.95	6.71
	CPGC-40	67.88	79.55	54.60	66.58	58.88	78.29	89.60	81.80	87.30	83.38	81.50	76.00	73.29	77.60	134.19
	DO-UAP (ours)	81.66	86.26	76.79	82.66	72.12	86.58	87.50	81.05	92.80	88.30	85.60	83.60	82.75	84.74	5.83
MSCOCO	GAP	93.91	91.82	87.93	86.98	60.09	66.84	91.17	85.99	89.00	80.67	71.10	76.95	82.20	81.54	5.21
	CPGC-2	89.89	92.15	86.94	87.00	75.47	76.25	86.16	72.42	90.30	80.75	71.49	71.29	83.38	79.98	6.51
	CPGC-40	95.81	95.55	89.42	85.81	90.73	92.46	94.31	89.33	95.23	89.27	91.97	90.21	92.91	90.44	130.13
	DO-UAP (ours)	94.13	93.98	91.99	95.29	76.57	78.57	96.59	92.21	95.68	91.70	90.78	94.30	90.96	91.01	5.63

A Appendix / supplemental material

A.1 More Results on ITR Task

We present experimental results of the ITR task on R@5 and R@10 in Table 11 and Table 12. We report the attack success rate (higher is better) on R@5 and R@10, where R@N denotes the top N most relevant text or image matches based on the query. In summary, our DO-UAP method surpasses CPGC in attack performance with an average improvement of 4.07% on the TR task and 3.79% on the IR task across both Flickr30K and MSCOCO datasets. The results are consistent with those in Sec. 4.2.